Investigation of jet break-up process in diesel engine Spray modelling

M.H. Djavareshkian[1], V. Pirouzpanah[2] and A. Ghasemi[3]

Department of Mechanical Engineering, University of Tabriz, IRAN

Eng_mech78@yahoo.com

Abstract

Fluid mechanical or CFD simulation is playing an increasingly important role in the simulation of engine processes, as it makes possible the most detailed physical description of the relevant processes. The objective of this work is to simulate spray flow with different break-up models and investigate the effect of these models on DI diesel engine combustion and performance. In this simulation, the 3-Dimensional Naiver-Stokes equation is solved with SIMPLEC algorithm. An eddy break-up combustion model and a diesel auto-ignition model were implemented to simulate the ignition and combustion process in a diesel engine. All the simulations were carried out by the use of FIRE CFD tool. Results were validated with available experimental data for OM_355 DI diesel engine for mean cylinder pressure. The results show that there have been good agreements between experiments and the CFD calculations. The research demonstrated that multidimensional modeling is useful for diesel engine spray modeling and optimization.

Keywords: Breakup-Diesel engine-Sauter Mean Diameter-Penetration

1. Introduction

In the last decade 3D-CFD has been successfully established for three dimensional simulations of fluid flow, mixture formation, combustion, and pollutant formation in internal combustion engines. In direct injected engines the accuracy of the simulation results and hence their contribution to design analysis and optimization strongly depends on the predictive capabilities of the models adopted for simulation of the injector flow, spray formation and propagation characteristics [1-7]. Since experiments can be difficult to manage for injection conditions (small-scaled, high-speed flow) [8], a numerical simulation seems to be an appropriate tool to get an interesting model of the flow features inside and at the exit of the injector nozzle. The knowledge of the injector mass flow rate and the flow conditions at the nozzle exit can be a key issue for a successful simulation of all the subsequent processes of mixture formation, and eventually combustion and pollutant formation [9]. Spray simulations involve multi-phase flow phenomena and as such require the numerical solution of conservation equations for the gas and the liquid phase simultaneously. With respect to the liquid phase, practically all spray calculations in the engineering environment today are based on a statistical method referred to as the *Discrete Droplet Method (DDM)* [10]. This operates by solving ordinary differential equations for the trajectory, momentum, heat and mass transfer of single droplets, each being a member of a group of identical non-interacting droplets termed a '*parcel*'. Thus one member of the group represents the behavior of the complete parcel. Droplet parcels are introduced in the flow domain with initial conditions of position, size, velocity, temperature and number of particles in the parcel. FIRE supports the introduction of droplets, emerging from a nozzle as a spray and entering the flow domain through the inlet areas as a gas/liquid mixture. The atomization process of sprays is accounted for with distinctive submodels. The droplet-gas momentum exchange, turbulent dispersion, evaporation of droplets, secondary break-up, droplet collision and droplet-wall interaction are covered with a comprehensive set of models which allow the usage of the module for many different flow regimes. The vapor of evaporating droplets is used as a source term of an additional transport equation for the vapor void fraction in Eulerian formulation. [9]. Primary/secondary break-up modeling that accounts for the competing effects of turbulence, cavitation and aerodynamic induced break-up processes is based upon the spatially and temporally resolved injector flow data at the nozzle exit. In reference [11] the turbulence induced break-up is accounted for by solving a transport equation for the turbulent kinetic energy and its dissipation rate within the liquid fuel core. The impact of the collapsing cavitation bubbles on the primary break-up is modeled via additional source terms in the turbulence model. The turbulence and cavitation induced break-up competes with the aerodynamic one until at a certain distance downstream of the nozzle exit the aerodynamic break-up

---

[1] Associate prefessor, Fluid mechanics
[2] Professor, combustion
[3] M.S. student, combustion

processes become dominant [11]. It is evident that the maximum turbulence / cavitation induced break-up intensity is observed very close to the nozzle exit and can be attributed to the nozzle flow induced and (to a minor extent) to the cavitation collapse induced turbulent velocity fluctuations [11]. Due to dissipation of the turbulent fluctuations, however, the turbulence induced break-up rate is significantly reduced with increasing distance from the nozzle exit until it becomes negligible at about 2.5 mm downstream of the nozzle tip. The aerodynamic break-up rates show the opposite behavior, i.e. they are very low immediately at the nozzle exit but increase significantly with increasing distance from the nozzle, where the compact liquid core has already been significantly disintegrated due to primary break-up mechanisms. Finally, even at the spray axis high aerodynamic break-up rates can be identified, indicating complete fragmentation of the compact spray core [11]

Elevated injection pressure levels lead to higher injection velocities and hence increased turbulence levels which directly lead to higher turbulence induced break-up rates. Increased chamber back-pressure levels, however, affect mainly the aerodynamic break-up mechanisms via the impact of higher gas densities and hence elevated interaction forces between ligaments / droplets and gaseous phase [11]

The present article provides an overview of the proper boundary conditions and models required for successful simulation of the spray formation/propagation characteristics in direct injected diesel engines. Individual model results are validated against selected experimental data. For all cases presented in this study the CFD code FIRE is used for simulation of the relevant injector flow and spray formation and propagation processes.

2. Basic Equations

The conservation equations are presented for the following dynamic and thermodynamic properties [9]:
• Mass →Equation of Continuity

$$\frac{\partial \hat{\rho}}{\partial t} = -\frac{\partial}{\partial x_j}\left(\hat{\rho}\hat{U}_j\right) \tag{1}$$

• Momentum (Newton's second law) → Navier-Stokes Equations

$$\frac{D(\hat{\rho}\hat{U})}{Dt} = \frac{\partial(\hat{\rho}\hat{U}_i)}{\partial t} + \frac{\partial(\hat{\rho}\hat{U}_j\hat{U}_i)}{\partial x_j}$$

$$= \hat{\rho}g_i - \frac{\partial \hat{P}}{\partial x_i} + \frac{\partial}{\partial x_j}\left[\mu\left(\frac{\partial \hat{U}_i}{\partial x_j} + \frac{\partial \hat{U}_j}{\partial x_i} - \frac{2}{3}\frac{\partial \hat{U}_k}{\partial x_k}\delta_{ij}\right)\right] \tag{2}$$

• Energy (1st Law of Thermodynamics) → Equation of Energy

$$\frac{D(\hat{\rho}\hat{H})}{Dt} = \frac{\partial(\hat{\rho}\hat{H})}{\partial t} + \frac{\partial(\hat{\rho}\hat{U}_j\hat{H})}{\partial x_j}$$

$$= \hat{\rho}\dot{q}_g + \frac{\partial \hat{P}}{\partial t} + \frac{\partial}{\partial x_i}\left(\hat{\tau}_{ij}\hat{U}_j\right) + \frac{\partial}{\partial x_j}\left(\lambda\frac{\partial \hat{T}}{\partial x_j}\right) \tag{3}$$

• Concentration Equation

$$\frac{D(\hat{\rho}\hat{C})}{Dt} = \frac{\partial(\hat{\rho}\hat{C})}{\partial t} + \frac{\partial(\hat{\rho}\hat{U}_j\hat{C})}{\partial x_j}$$

$$= \hat{\rho}\dot{r} + \frac{\partial \hat{P}}{\partial t} + \frac{\partial}{\partial x_j}\left(D\frac{\partial \hat{C}}{\partial x_j}\right) \tag{4}$$

3. Numerical Calculation Method

The AVL FIREv8.5 CFD tool was implemented to simulate diesel engine combustion with special focus on break-up process modeling. FIRE solves unsteady compressible turbulent reacting flows by using finite volume method. Turbulent flow in the combustion chamber was modeled with $k-\varepsilon$ turbulence model. An eddy break-up combustion model was implemented to simulate the combustion process in a diesel engine. The reaction mechanism used for the simulation of the auto-ignition of the diesel fuel is based upon an extended version of the well known SHELL model.

In this paper, different break-up models such as WAVE, FIPA, & KH-RT were utilized and their effect on combustion was investigated.

4. Computational Grid Generation

Based on the geometry description, a set of computational meshes covering 360°CA is created. The mesh generation process is divided into the creation of 2D and 3D mesh. The 2D mesh of the modeled engine is shown in Fig. 1. The angle of the computational sector is 90 degrees. This mesh resolution has been found to provide adequately independent grid results. The multi-block structure of the grid, containing spray and injector blocks, is shown in figure 2.
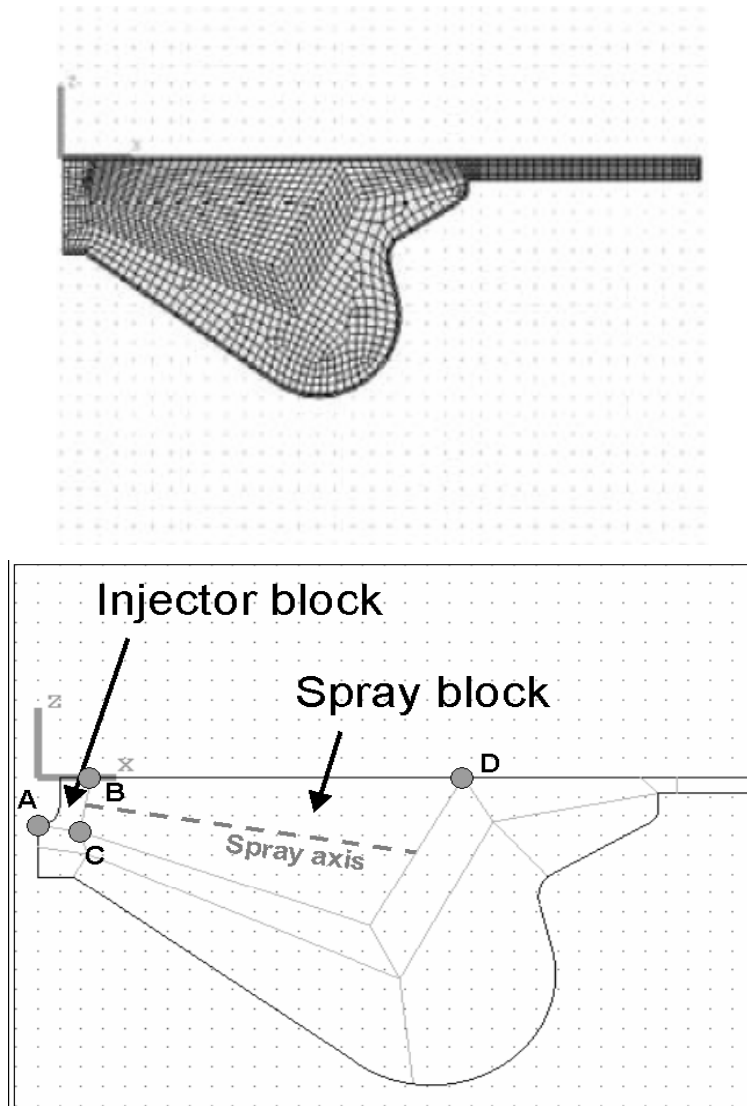

Figure 2: Multi-block structure of the grid

5. Overview of Typical Boundary Conditions

The wall (surface) temperatures (cylinder liner, cylinder head, piston) are based on experimental experiences and depend on the operating point (load and speed). The boundary conditions of the cylinder head are specified as fixed wall, the boundary conditions of the piston bowl as moving wall. In figure 3, overview of the selected boundary conditions is shown.
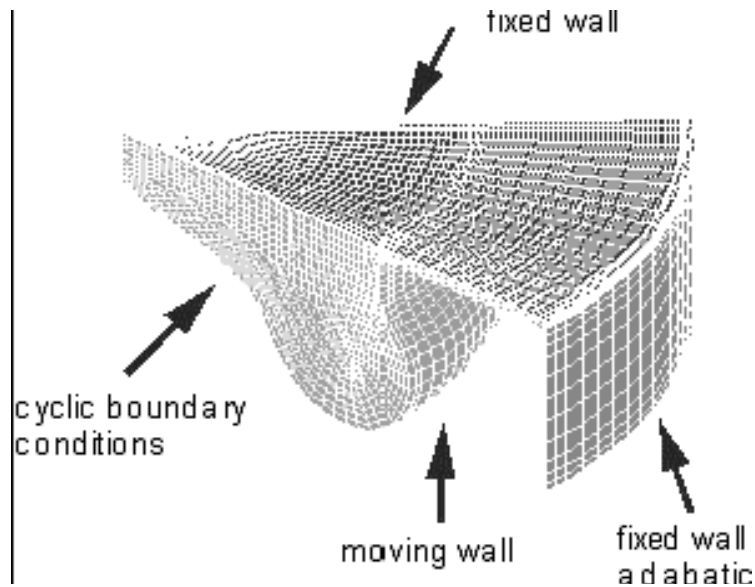
Figure 3: Boundary Conditions – Overview

Symmetry boundary conditions are applied to the radius surface along the center axis of the segment mesh. This symmetry boundary conditions might cause problems with calculation results regarding temperature. In this case adiabatic fixed wall boundary conditions can be specified. In figure 4 details of the boundary conditions is shown.
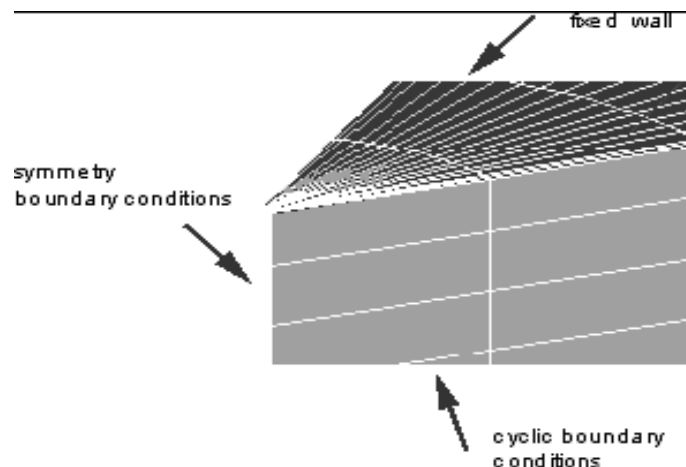

Figure 3: Boundary Conditions – details

The boundary conditions concerning the additional compensation volume are applied in this way. Faces at the outer, inner and lower side of the volume are specified as moving wall adiabatic (heat flux =0). Figure 4 shows the moving wall adiabatic boundary conditions.
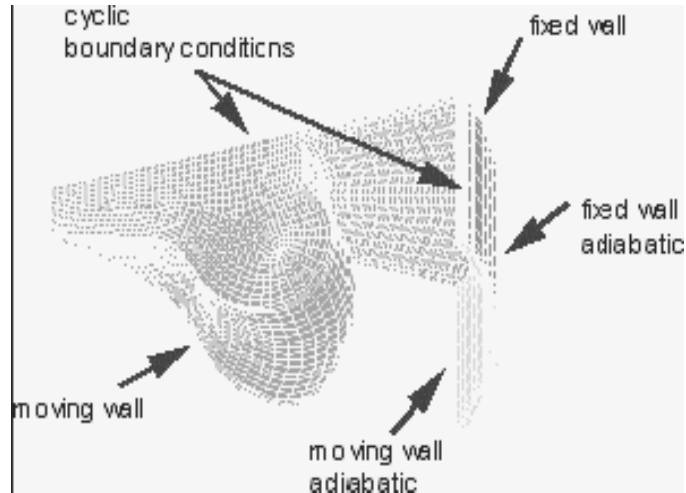
Figure 4: Moving Wall Adiabatic Boundary Conditions

The faces in polar direction are specified as cyclic boundary conditions. Figure 5 shows selections for cyclic boundary conditions.
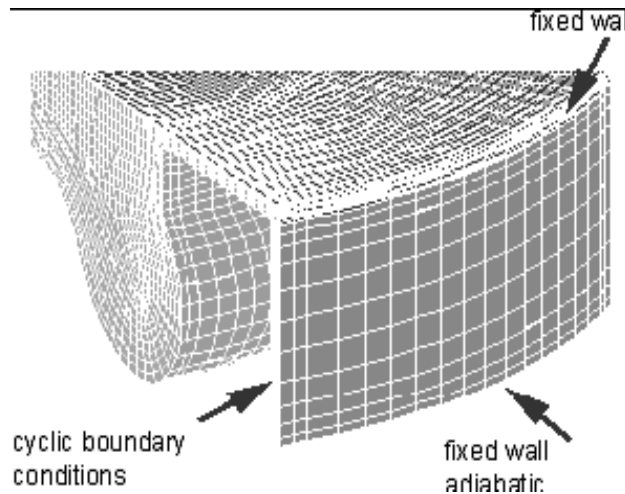

Figure 5: Selections for cyclic boundary conditions.

6. Engine Specifications and Operating Conditions

The OM355 Mercedes Benz diesel engine is used in this simulation. The specifications of mentioned engine are shown in Table 1.

TABLE 1: OM-355 Engine Specifications and Operating Conditions

Engine model	OM-355
Number of cylinders	6
Bore	128 (mm)
Stroke	150 (mm)
Compression ratio	16.1:1
Intake pressure	99 (kpa)
Intake temperature	300 (K)
Engine speed	1400 (RPM)
Air/Fuel ratio	18.5
Beginning of injection	18.5 (BTDC)
Measured power	116.1 (kpa)

7. Spray Model

Currently the most common spray description is based on the Lagrangian discrete droplet method [12]. While the continuous gaseous phase is described by the standard Eulerian conservation equations, the transport of the dispersed phase is calculated by tracking the trajectories of a certain number of representative parcels (particles). A parcel consists of a number of droplets and it is assumed that all the droplets within one parcel have the same Physical properties and behave equally when they move, break-up, hit a wall or evaporate. The coupling between the liquid and the gaseous phases is achieved by source term exchange for mass, momentum, energy and turbulence. Various sub-models account for the effects of turbulent dispersion [13], coalescence [14], evaporation [15], wall interaction [11] and droplet break up [14].

7.1. Spray Model Equations

The differential equations for the trajectory and velocity of a particle parcel are as follows [9]:

-Momentum

$$m_d \frac{dU_{id}}{dt} = F_{idr} + F_{ig} + F_{ip} + F_{ib} \tag{5}$$

Where F_{idr} is the drag force, given by :

$$F_{idr} = D_p . u_{irel} \tag{6}$$

D_p is the drag function, defined as:

$$D_p = \frac{1}{2} \rho_g A_d C_D |u_{rel}| \tag{7}$$

C_D is the drag coefficient which generally is a function of the droplet Reynolds number Re_d and A_d is the cross-sectional area of the particle.

From the various formulations in literature for the drag coefficient of a single sphere, FIRE uses the formulation from Schiller and Naumann [16].

F_{ig} is a force including the effects of gravity and buoyancy :

$$F_{ig} = V_p . (\rho_p - \rho_g) g_i \tag{8}$$

F_{ip} is the pressure force, given by :

$$F_{ip} = V_p . \nabla p \tag{9}$$

F_{ib} summarizes other external forces like the so-called virtual mass force, magnetic or electrostatic forces, Magnus force or others.

Therefore, inserting above forces and relations into equation (5) and dividing it by the particle mass m_d the equation for the particle acceleration as used by default is :

$$\frac{du_{id}}{dt} = \frac{3}{4} C_D \frac{\rho_g}{\rho_d} \frac{1}{D_d} |u_{ig} - u_{id}| (u_{ig} - u_{id}) + \left(1 - \frac{\rho_g}{\rho_d}\right) g_i \tag{10}$$

Which can be integrated to get the particle velocity and from this the instantaneous particle position vector can be determined by integrating:

$$\frac{dX_{id}}{dt} = u_{id} \tag{11}$$

8. Break-Up Modelling

The atomization of diesel engine fuel sprays can be divided into two main processes, primary and secondary break-up. The former takes place in the region close to the nozzle at high Weber numbers. It is not only determined by the interaction between the liquid and gaseous phases but also by internal nozzle phenomena like turbulence and cavitation. Atomization that occurs further downstream in the spray due to aerodynamic interaction processes and which is largely independent of the nozzle type is called secondary break-up.

The classic break-up models like TAB (Taylor Analogy Break-up), RD (Reitz and Diwakar) and WAVE do not distinguish between the two processes [15]. The parameters of these models are usually tuned to match experimental data further downstream in the region of the secondary break-up. Originally, these parameters are supposed to depend only on nozzle geometry, in reality they also account for numerical effects.

Other models like ETAB (Enhanced TAB), FIPA (Fractionnement Induit Par Acceleration) or KH-RT (Kelvin Helmholtz - Rayleigh Taylor) treat the primary break-up region separately [15]. Hence, they in principle offer the possibility to simulate both break-up processes independently. The correct values for the additional set of parameters, however, are not easy to determine due to the lack of experimental data for the primary break-up region.

Despite the sometimes tedious tuning of these model parameters the use of break-up models is generally advantageous compared to the initialization of measured droplet distributions at the nozzle orifice. In the first approach the droplets are simply initialized with a diameter equal to the nozzle orifice (blob injection), the droplet spectrum automatically evolves from the subsequent break-up processes. The latter approach gives satisfying results only as long as injection pressure and droplet Weber numbers are low [17].

In this work we will investigate the WAVE, FIPA, & KH_RT break-up models. Here we give an overview of these models.

8.1. WAVE Standard

The growth of an initial perturbation on a liquid surface is linked to its wavelength and to other physical and dynamic parameters of the injected fuel and the domain fluid [18].

There are two break-up regimes, one for high velocities and one for low velocity Rayleigh type break-up. For the first case the size of the product droplets is set equal to the wavelength of the fastest growing or most probable unstable surface wave. Rayleigh type break-up produces droplets that are larger than the original parent drops. This regime is not important for high pressure injection systems.

As for the Reitz-Diwakar model also for the Wave model a rate approach for the radius reduction of the parent drops is applied:

$$\frac{dr}{dt} = -\frac{(r - r_{stable})}{\tau_a} \tag{12}$$

Where τ_a is the break-up time of the model, which can be calculated as:

$$\tau_a = \frac{3.726.C_2.r}{\Lambda.\Omega} \tag{13}$$

The constant C_2 corrects the characteristic break-up time and varies from one injector to another. r_{stable} is the droplet radius of the product droplet, which is proportional to the wavelength Λ of the fastest growing wave on the liquid surface.

$$r_{stable} = C_1\Lambda \tag{14}$$

The recommended default value of C_1 taken from the original paper of Reitz is 0.61. The wave length Λ and wave growth rate Ω depend on the local flow properties.

$$\Lambda = 9.02.r \frac{(1 + 0.45.Oh^{0.5})(1 + 0.4.T^{0.7})}{(1 + 0.87.We_g^{1.67})^{0.6}} \tag{15}$$

$$\Omega = \left(\frac{\rho_g r^3}{\sigma}\right)^{-0.5} \frac{0.34 + 0.38.We_g^{1.5}}{(1 + Oh)(1 + 1.4.T^{0.6})} \tag{16}$$

Entering Reynolds Re and Ohnesorge number Oh as well as $T = Oh.We^{0.5}$.

8.2. FIPA

The authors of this model assume that primary and secondary break-up have to be treated separately [19]. As the WAVE model was developed from the analysis of perturbations on liquid surfaces it is used for primary break-up. For secondary break-up the experimentally determined equations by Pilch and Erdman [20] are applied:

$$\tau_{bu} = 6.00(We - 12)^{-0.25} \qquad 12 < We < 18$$

$$\tau_{bu} = 2.45(We - 12)^{+0.25} \qquad 8 < We < 45$$

$$\tau_{bu} = 14.1(We - 12)^{-0.25} \qquad 45 < We < 351 \qquad (17)$$

$$\tau_{bu} = .766(We - 12)^{+0.25} \qquad 351 < We < 2670$$

$$\tau_{bu} = 5.5 \qquad 2670 < We$$

τ_{bu} is the non-dimensionalized break-up time for inviscid liquids. The transition from primary to secondary break-up is arbitrarily set at We = 1000. This time the Weber number is calculated with the diameter and not with the radius. To get the break-up time τ for the secondary break-up the following relation is needed:

$$\tau = C_{23} . \tau_{bu} . \sqrt{\frac{\rho_l}{\rho_g} . \frac{d}{V_r}} \qquad (18)$$

The factor C_{23} is a constant similar to C_2 in the Wave model. C_{23} is a function of the void fraction and the constants C_2 and C_3. The idea is that the break-up process is reduced in cells where the spray is densely packed. C_2 is valid for void fractions bigger than 0.99999, C_3 for void fractions less than 0.99, values in between are interpolated.

As in the Wave model, the characteristic break-up time and the stable droplet radius control the gradual break-up process.

$$\frac{dr}{dt} = -\frac{(r - r_{stable})}{(\tau - \tau_s)^{C_6}} \qquad (19)$$

Contrary to the other models there is an exponential factor C_6, and the characteristic break-up time τ is calculated only once at the beginning of the break-up. τ_s is the elapsed time since the calculation of τ.

8.3. KH-RT

In this model Kelvin-Helmholtz (KH) surface waves and Rayleigh-Taylor (RT) disturbances should be in continuous competition of breaking up the droplets [21], [22].

The KH mechanism is favored by high relative velocities and high ambient density. The RT mechanism is driven by rapid deceleration of the droplets causing growth of surface waves at the droplet stagnation point. The WAVE model equations [23]

$$R_a = C_1 \Lambda$$

$$\tau_a = \frac{3.7 C_2 R}{\Lambda \Omega}$$

$$\Lambda = f(We_c, Oh_d) \qquad (20)$$

$$\Omega = f(We_c, Oh_d)$$

Simulate the KH break-up. We_c is indicating continuous phase properties and Oh_d is indicating droplet properties.

The RT disturbances are described by the fastest growing frequency Ω and the corresponding wave number K.

$$\Omega_t = \sqrt{\frac{2}{3\sqrt{3\sigma}} \frac{g_t |(\rho_d - \rho_c)|^{1.5}}{\rho_d + \rho_c}} \qquad \tau_t = C_5 \frac{1}{\Omega_t} \qquad (21)$$

$$K_t = \sqrt{\frac{g_t |\rho_d - \rho_c|}{3\sigma}} \qquad \Lambda_t = C_4 \frac{\pi}{K_t} \qquad (22)$$

Here g is the deceleration in the direction of travel. If the wave length Λ is small enough to be growing on the droplet's surface and the characteristic RT break-up time τ has passed, the droplets atomize and their new sizes are assumed to be proportional to the RT wave length. Droplets within the break-up length L

$$L = C_3 \sqrt{\frac{\rho_d}{\rho_c}} d_o \qquad (23)$$

are considered to undergo only KH break-up, whereas further downstream both mechanisms are present. If desired also child droplets can be created by using model parameters C_6 and C_7. Parameter C_6 determines the fraction of the parcel volume which has to be detached until child parcels are initialized, while C_7 determines the fraction of the shed mass which is finally transformed into child parcels. Thus it is possible to adjust frequency by C_6 and mass of child parcels by C_7 independently. The normal velocity component given to the child parcels is calculated from disturbance wavelength and growth rate modified by model parameter C_8.

9. Results and discussion

Figure 6 shows the comparison of mean cylinder pressure for present calculation and experimental data [25]. As can be seen, the agreement between two results is very good.
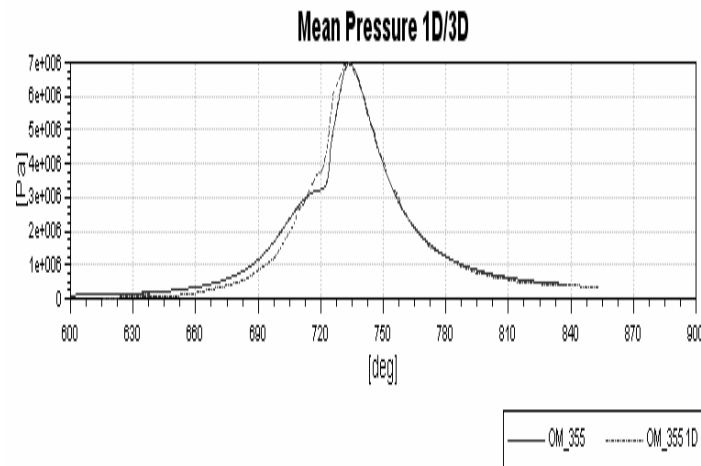

Figure 6 Comparison of Cylinder pressure for Model (Continuous) and experiment[25] (dashed)

The introduction of break-up models has considerably simplified the simulation of spray processes. In the past a number of different approaches have been presented and it is not easy to decide which one to choose for a specific simulation task. It turns out that practically all the break-up models are capable of reproducing measured data, as long as model constants are properly chosen.

According to reference [24], the time-dependent development of the spray penetration length can be divided into two phases. The first phase starts at the beginning of injection ($t = 0$, needle begins to open) and ends at the moment the liquid jet emerging from the nozzle hole begins to disintegrate $(t = t_{break})$. Because of the small needle lift and the low mass flow at the beginning of injection, the injection velocity is small, and the first jet break-up needs not always occur immediately after the liquid leaves the nozzle. During the second phase $(t \rangle t_{break})$, the spray tip consists of droplets, and the tip velocity is smaller than during the first phase. The spray tip continues to penetrate into the gas due to new droplets with high kinetic energy that follow in the wake of the slower droplets at the tip (high exchange of momentum with the gas) and replace them. Experimental investigations have shown that the transition from a pure turbulent to a cavitating nozzle hole flow results in an increase of spray cone angle and in a decrease of penetration length. Strongly cavitating nozzle flows produce larger overall spray cone angles and smaller penetration lengths than non-cavitating ones.

The spray penetration increases with time due to the effect that new droplets with high kinetic energy continuously replace the slow droplets at the spray tip.

Figure 7 shows the comparison of different break-up models for Sauter Mean Diameter (a), & spray penetration (b). The penetration depth shows the temporal development of the path of the spray tip in the combustion chamber. In the case of spray penetration in figure 2 there is no increase with time, it is because we have set the injection rate to 1. It means that at the beginning of the injection period (injector needle lift), the spray tip reaches it's maximum penetration and remains approximately constant during the injection.

One quantity characterizing the average droplet is size of a spray and thus the success of spray break-up is the Sauter mean diameter (SMD).

d32-Sauter diameter
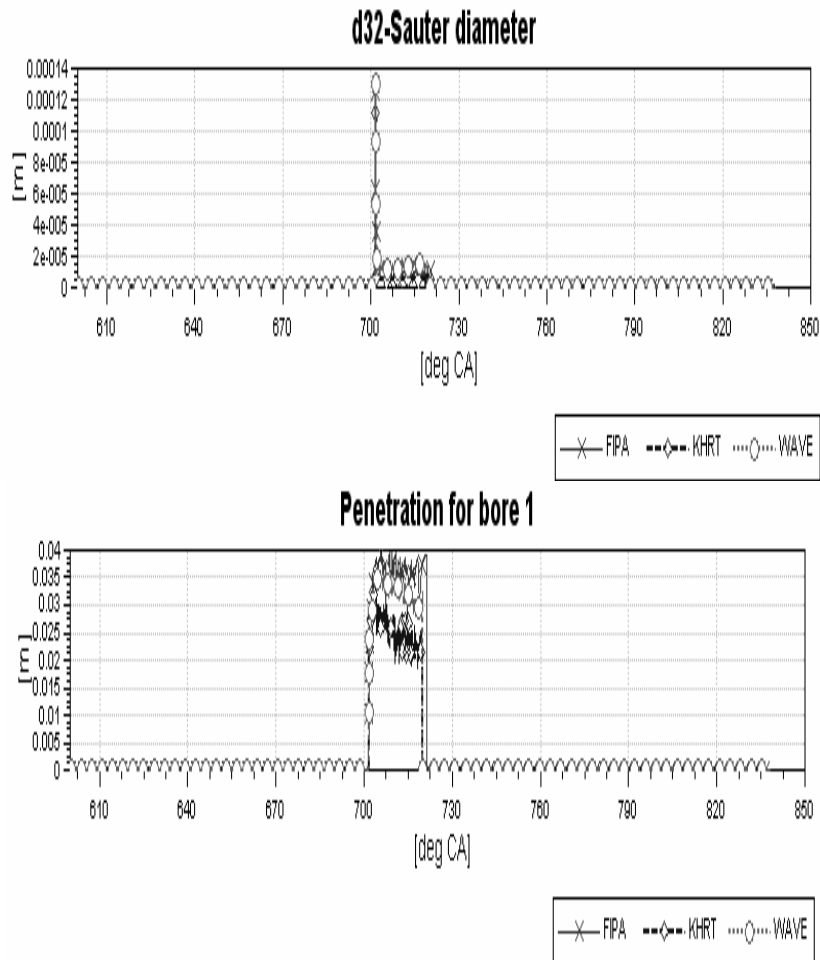

Penetration for bore 1

Figure 7 Comparison of different break-up models; a) Sauter Mean Diameter, b) spray penetration

Figure 8 presents the effect of different break-up models on the amount of liquid mass remaining after injection. If standard WAVE model with blob injection (=> initial droplets have the diameter of the nozzle orifice) is used for the simulation, it often happens that there is hardly any fuel vapor close to the nozzle. This is due to the fact that the droplets are still very large at the beginning and therefore hardly evaporate.

The longer the penetration length, The smaller the energy of the new droplets at the tip and the slower the tip velocity. A higher injection pressure results in increased penetration, while an increase in gas density reduces penetration. An increase in the nozzle diameter increases the momentum of the jet and increases penetration. The KH-RT model with the lower penetration exhibits the most amount of liquid remaining.
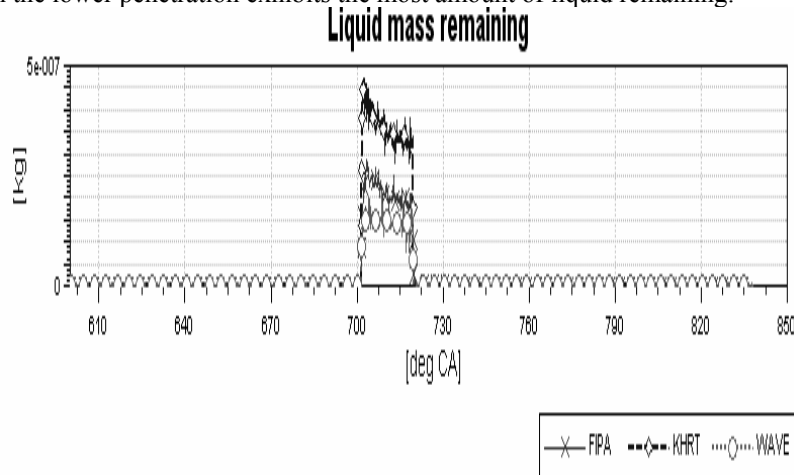
Liquid mass remaining

Figure 8 Liquid mass remaining

Figure 9 represents the effect of different break-up models on the mean cylinder pressure. This figure shows that the results of the FIPA and WAVE models are similar, and the KH-RT model with higher remained fuel exhibits higher cylinder peak pressure.
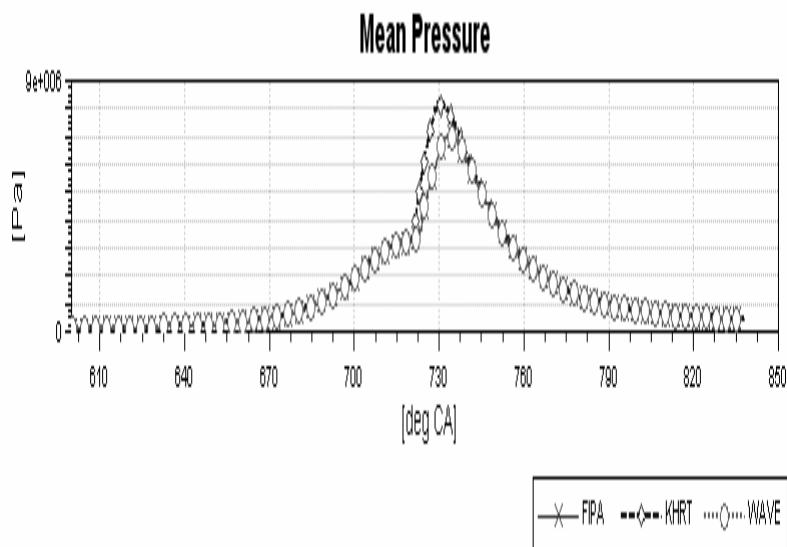
Mean Pressure

Figure 9 Comparison of cylinder pressure for different Breakup models.

Figure 10 represents the effect of different break-up models on the combustion rate or heat release rate. This figure shows again the similarity between the results of FIPA and WAVE models in predicting the heat release rate. As it can be seen the KH-RT model that has predicted higher amount of remaining fuel, reduced penetration, increased spray disintegration, and correspondingly faster fuel-air mixing. This condition causes more premixed combustion, and correspondingly leads to higher cylinder peak pressure.
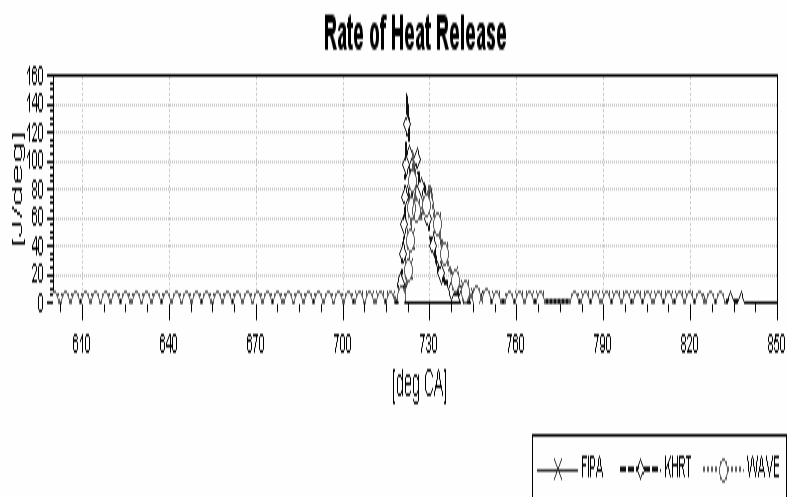
Rate of Heat Release

Figure 10 Comparison of Heat release rate for different breakup models.

Figure 11 describes the variation of the Sauter Msean Diameter (SMD) distribution during the injection process in different break-up models. For all models it is obvious that the SMD has greater amounts near the nozzle hole, and will become smaller far from the nozzle exit due to breakup process. The smaller the SMD, the more surface per unit volume. The more surface, the more effective evaporation and mixture formation. Although the SMD is a well known quantity in characterizing the spray formation process, it is important to remember that it does not provide any information about the droplet size distribution of the spray. In other words, two sprays with equal SMD can have significantly different droplet size distributions.
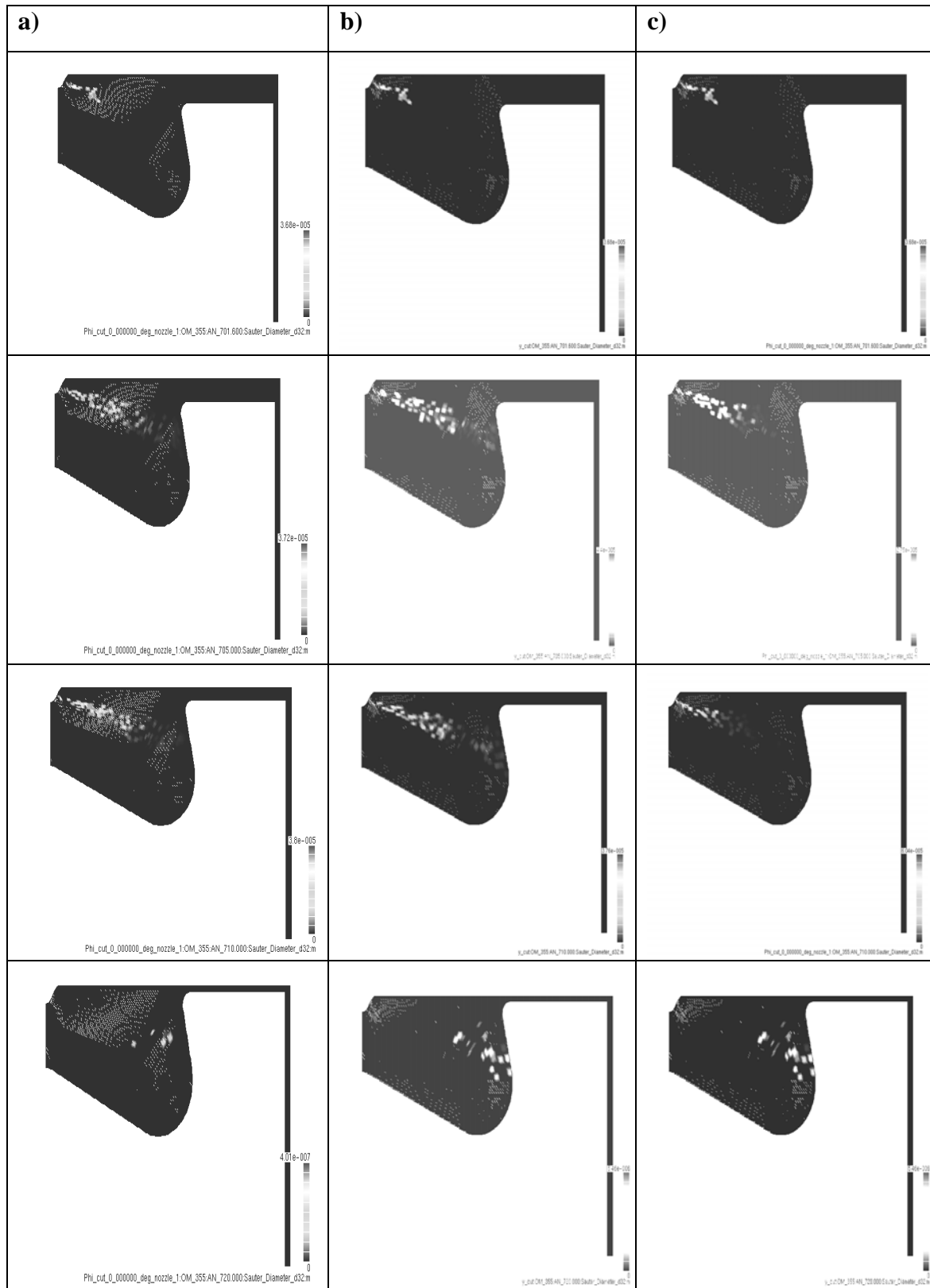
a)   b)   c)

Figure 11 Comparison of SMD in four crank angles (701.6, 705, 710 and 720ºCA) for different breakup models: a) WAVE b) FIPA c) KH-RT

9.1. Main results

From the study on the diesel engine spray break-up using three different break-up models, the following conclusions may be drawn:

1- The research demonstrated that multidimensional modeling is useful for diesel engine spray modeling and optimization.
2- The knowledge of the injector mass flow rate and the flow conditions at the nozzle exit can be a key issue for a successful simulation of all the subsequent processes of mixture formation, and eventually combustion and pollutant formation
3- It turns out that practically all the break-up models are capable of reproducing measured data, as long as model constants are properly chosen.
4- The KH-RT model that has the higher amount of remaining fuel, predicts more premixed combustion, and correspondingly this leads to higher cylinder peak pressure.
5- For all models it is obvious that the SMD has greater amounts near the nozzle hole.
6- An increase in penetration can be due to reduced break-up.
7- Reduced penetration, increased spray disintegration, and correspondingly faster fuel-air mixing causes more premixed combustion, and correspondingly leads to higher cylinder peak pressure.

10. Conclusions

In the present article the spray flow has been simulated with different break-up models and the effect of these models on DI diesel engine combustion and performance was investigated. All the simulations were carried out by the use of FIRE CFD tool. Results were validated with available experimental data for OM_355 DI diesel engine for mean cylinder pressure. There have been good agreements between experiments and the CFD calculations.

REFERENCES

[1] Tatschl, R., Wieser, K., Reitbauer, R., Multidimensional Simulation of Flow Evolution, Mixture Preparation and Combustion in a 4-Valve Gasoline Engine, COMODIA 94, Yokohama, 1994
[2] Tatschl, R., Fuchs, H., Brandstätter, W. Experimentally Validated Multi-dimensional Simulation of Mixture Formation and Combustion in Gasoline Engines, IMechE C499/050/96, 1996
[3] Tatschl, R., Riediger, H., PDF Modeling of Stratified Charge SI Engine Combustion, SAE 981464, 1998
[4] Tatschl, R., Pachler, K., Winklhofer, E., A Comprehensive DI Diesel Combustion Model for Multidimensional Engine Simulation, COMODIA 98, Kyoto, 1998
[5] Tatschl, R., Riediger, H., Bogensperger, M., Multidimensional Simulation of Spray Combustion and Pollutant Formation in a Medium Speed Marine Diesel Engine, 1998 FISITA World Automotive Congress, Paris, 1998
[6] Tatschl, R., Wiesler, B., Alajbegovic, A., Kuensberg Sarre, Ch., Advanced 3D Fluid Dynamic Simulation for Diesel Engines, Thermofluidynamic Processes in Diesel Engines, Valencia, 2000
[7] Tatschl, R., Riediger, H., v. Künsberg Sarre, Ch., Putz, N., Fast Grid Generation and Advanced Physical Modelling – Keys to Successful Application of CFD to Gasoline DI Engine Analysis, ImechE C587/042/2000, 2000
[8] Ueki, H., Ishida, M. and Sakaguchi, D, "Investigation of droplet disintegration in diesel spray core by Advanced Laser 2-Focus velocimeter", SAE Paper No. 2005-01-1238.
[9] FIRE v8.5 Manuals AVL List GmBH.
[10] Dukowicz, J.K. "A Particle-Fluid Numerical Model for Liquid Sprays", J. Comp. Physics, 35, 229-253, 1980.
[11] Naber, J.D., Reitz, R.D., Modeling Engine Spray / Wall Impingement, SAE 880107, 1988
[12] Dukowicz, J.K., A Particle-Fluid Numerical Model for Liquid Sprays, Journal of Computational Physics, Vol. 35, pp. 229-253, 1980
[13] Gosman A.D. and Ioannides, E., Aspects of Computer Simulation of Liquid-Fueled Combusters, J. Energy, 7, pp. 482 490, 1983
[14] O'Rourke, P.J., Modeling of Drop Interaction in Thick Sprays and a Comparison with Experiments, IMechE - Stratified Charge Automotive Engines Conference, 1980
[15] Dukowicz, J.K., Quasi-steady Droplet Phase Change in the Presence of Convection, Los Alamos Report LA-7997-MS, 1979
[16] Schiller, L. and Naumann, A. Z., VDI 77, 318-320 (1933)
[17] Reinhard TATSCHL, Christopher v. KÜNSBERG SARRE and Eberhard v. BERG, IC-ENGINE SPRAY MODELING – STATUS AND OUTLOOK, International Multidimensional Engine Modeling User's Group Meeting at the SAE Congress 2002.
[18] Liu, A.B. and Reitz, R.D. "Modeling the Effects of Drop Drag and Break-up on Fuel Sprays", SAE 930072.
[19] Baritaud, T. "Modeling Atomization and Break-up in High-Pressure Diesel Sprays", SAE 970881.
[20] Pilch, M. and Erdman, C.A. "Use of Break-up Time Data and Velocity History Data to Predict the Maximum Size of Stable Fragments for Acceleration-induced Breakup of a Liquid Drop", International Journal Multiphase Flow, Vol. 13, 1987.

[21] Su, T.F., Patterson, M.A., Reitz, R.D. and Farrell, P.V. "Experimental and Numerical Studies of High Pressure Multiple Injection Sprays", SAE 960861, 1996.

[22] v. Künsberg-Sarre, C. and Tatschl, R. "Spray Modelling / Atomisation – Current Status of Break-up Models", IMECHE-Seminar, December 15-16, 1998, The Lawn, Lincoln, UK.

[23] Reitz, R.D. and Bracco, F.V. "Mechanism of Atomization of a Liquid Jet", Physic of Fluids 25 (10), 1982.

[24] Hiroyasu H, Arai M (1990) Structures of Fuel Sprays in Diesel Engines. SAE-paper 900475

[25] Pirouzpanah V et al, ``Reduction of pollutants emissions of OM_355 diesel engine to Euro 2 by convecting to dual fuel engine (diesel + gas) .In: Proceeding of first conference of conversion automotive fuel to CNG , 19-20 june 2003, Tehran Iran .p.84-94.